HHS Public Access

Author manuscript

Dev Cell. Author manuscript; available in PMC 2016 March 23.

Published in final edited form as:

Dev Cell. 2015 March 23; 32(6): 667–677. doi:10.1016/j.devcel.2015.01.023.

Submandibular parasympathetic gangliogenesis requires Sprouty-dependent Wnt signals from epithelial progenitors

Wendy M. Knosp[1,#], **Sarah M. Knox**[1,2,#], **Isabelle M.A. Lombaert**[1], **Candace L. Haddox**[1], **Vaishali N. Patel**[1], and **Matthew P. Hoffman**[1,*]

[1]Matrix and Morphogenesis Section, NIDCR, NIH, Bethesda, MD 20892, USA

[2]Department of Cell and Tissue Biology, UCSF, San Francisco, CA 94143, USA

Abstract

Parasympathetic innervation is critical for submandibular gland (SMG) development and regeneration. Parasympathetic ganglia (PSG) are derived from Schwann cell precursors that migrate along nerves, differentiate into neurons, and coalesce within their target tissue to form ganglia. However, signals that initiate gangliogenesis after the precursors differentiate into neurons are unknown. We found deleting negative regulators of FGF signaling, Sprouty1 and Sprouty2 (*Spry1/2DKO*), resulted in a striking loss of gangliogenesis, innervation and keratin 5-positive (K5+) epithelial progenitors in the SMG. Here we identify Wnts produced by K5+ progenitors in the SMG as key mediators of gangliogenesis. Wnt signaling increases survival and proliferation of PSG neurons and inhibiting Wnt signaling disrupts gangliogenesis and organ innervation. Activating Wnt signaling and reducing FGF gene dosage rescues gangliogenesis and innervation in both the *Spry1/2DKO* SMG and pancreas. Thus K5+ progenitors produce Wnt signals to establish the PSG-epithelial communication required for organ innervation and progenitor cell maintenance.

Keywords

Gangliogenesis; Wnt; Wnt4; Wnt7b; Wnt10a; FGF; Fgf10; Fgf7; parasympathetic; ganglion; submandibular gland; progenitor

INTRODUCTION

Organogenesis requires integrated development of epithelial, neuronal, mesenchymal and endothelial cells. In the murine SMG, the epithelium receives signals from two key signaling

Corresponding author: Matthew P. Hoffman, Matrix and Morphogenesis Section, NIDCR, NIH, Bethesda, MD 20892, USA., Telephone: 301-496-1660, mhoffman@mail.nih.gov.

[#]These authors contributed equally to this work.

Author Contributions

W.M.K., S.M.K. and M.P.H. designed the experiments. W.M.K., S.M.K., I.M.A.L., V.N.P., and C.L.H. performed the experiments. W.M.K., S.M.K., V.N.P. and M.P.H. analyzed data and wrote the paper.

sources to coordinate epithelial morphogenesis (Knosp et al., 2012): the condensed mesenchyme into which the epithelium invaginates and the PSG that envelops the primary epithelial duct and develops in parallel with the epithelium (Coughlin, 1975; Knox et al., 2010). Signals from the PSG are required for the maintenance of proximal K5+ progenitors, and reciprocal signaling between the PSG and the epithelium is essential for neuronal function and survival (Knox et al., 2010; Lombaert et al., 2013; Nedvetsky et al., 2014). In the absence of epithelial-neuronal communication organogenesis and regeneration after irradiation damage are impaired.

It was recently discovered that parasympathetic ganglia are derived from peripheral Schwann cell precursors that migrate along nerves to their target tissue to form both the glia and neurons of the ganglia (Dyachuk et al., 2014; Espinosa-Medina et al., 2014). Thus, the PSG in the SMG arises from Schwann cell precursors that migrate along the chorda tympani and differentiate into βIII-tubulin-expressing neurons (TUBB3+). The next critical step in parasympathetic gangliogenesis occurs when the PSG neurons coalesce around the primary duct to form the ganglion and establish communication with the developing epithelium. Despite this critical need for neuronal-epithelial signaling during organogenesis, the signals that induce gangliogenesis and establish epithelial-PSG communication are not known.

SMG organogenesis requires FGF signaling as deletion of murine *Fgfr2b* or its ligand *Fgf10* causes gland aplasia (De Moerlooze et al., 2000; Ohuchi et al., 2000), and mutations in human FGFR2 or FGF10 result in gland aplasia or hypoplasia (Entesarian et al., 2005; Milunsky et al., 2006). Key intracellular modulators of FGF signaling are Sprouty (Spry) proteins, which act as negative-feedback antagonists (Minowada et al., 1999; Tang et al., 2011; Yu et al., 2011). Deletion of both *Spry1* and *Spry2* (*Spry1/2DKO*) in the lung increases MAPK signaling downstream of FGF10, which alters mitotic spindle angle and airway shape (Tang et al., 2011). In addition, *Spry1/2* are essential for normal sensory innervation of the pharynx and *Spry1/2DKO* embryos have enlarged geniculate ganglia and reduced branchial innervation (Simrick et al., 2011). However, the mechanisms by which Spry1/2 regulate parasympathetic gangliogenesis are unknown.

Wnt signals are also important for SMG organogenesis. Analysis of Wnt reporter mice shows that Wnt signaling initially localizes to the mesenchyme surrounding the E12 SMG epithelium and the distal cap mesenchyme. At later stages (>E13.5) it localizes to the ductal epithelium where it is important for duct differentiation: inhibition of Wnt signaling impairs duct differentiation whereas inhibition of FGF signaling, which increases Wnt activity, drives duct differentiation (Patel et al., 2011). However, inhibition of Wnt signaling early in development, when signaling is restricted to the mesenchyme that includes the PSG, also impairs branching morphogenesis (Haara et al., 2011). However, the impact of loss of Wnt signaling on the PSG was not investigated.

Here, we analyzed the SMGs in *Spry1/2DKO* embryos and discovered a striking loss of parasympathetic gangliogenesis, depletion of K5+ progenitors, and reduced epithelial Wnt expression and signaling. We hypothesized that secreted factors from the primary epithelial duct may drive this process. Using a combination of molecular techniques and ex vivo organ culture we identified that Wnt signals from K5+ progenitors in the ductal epithelium

promotes gangliogenesis, in part by inducing neuronal proliferation and cell survival. Reducing *Fgf10* gene dosage in *Spry1/2DKO* embryos along with in utero Wnt activator treatment rescues gangliogenesis, organ innervation and K5+ progenitor cells. We propose that epithelial Wnt signals are required for gangliogenesis and to establish PSG-epithelial communication during organogenesis.

RESULTS

Epithelial Spry1/2 are required for SMG parasympathetic gangliogenesis

Spry1 and *Spry2* are normally expressed in the SMG epithelium and genetic deletion of *Spry1/2* disrupts epithelial development resulting in a wide primary duct (white lines) and abnormal branching morphogenesis (Figures 1A and 1B). Strikingly, parasympathetic ganglia were not observed in the *Spry1/2DKO* SMG (Figure 1B). Consistent with this, microarray analysis comparing *Spry1/2DHet* ($Spry1^{+/-}$;$Spry2^{+/-}$) with *Spry1/2DKO* SMGs showed that markers of parasympathetic nerves, *Vip*, *Tubb3* and *Phox2b*, were reduced in the *Spry1/2DKO* (Supplementary Table 1). However, condensed mesenchyme and TUBB3+ neurons were present indicating that neural crest migration and neuronal differentiation still occurred (Figure 1B, arrowhead). Furthermore, sensory innervation of the tongue was not disrupted by loss of *Spry1/2* (Figure S1A), suggesting that parasympathetic but not distant sensory ganglia were adversely affected.

K5+ progenitor cells are located in the primary epithelial duct during early SMG development (E11.5–13) and then during later development (E14 and E16) are located in both the ducts and endbuds (Figures 1C–E). K5+ cells lie in the basal layer of the epithelial duct, however in the *Spry1/2DKO* the remaining K5+ cells become dispersed within a disorganized duct epithelium (Figure 1D). Consistent with the PSG being required for progenitor maintenance, fewer K5+ cells were observed in E14 *Spry1/2DKO* SMGs compared to controls, and by E16, only a small number K5+ progenitors remain (Figure 1E, white arrowheads). To confirm that loss of the PSG in the *Spry1/2DKO* was not due to a role of Spry1/2 within the neural crest-derived mesenchyme and nerves we generated conditional *Spry1/2* knockouts using $Wnt1^{cre}$ (Chai et al., 2000). In these mutants, gangliogenesis, innervation of the SMG and epithelial morphogenesis were not affected (Figure S2B). We confirmed that Spry1/2 are required within the epithelium by generating conditional *Spry1/2* knockouts using both Shh^{cre} and $K14^{cre}$ (Shh^{cre};$K14^{cre}$;$Spry1/2^{fl/-}$), which are expressed in 80 +/− 4 percent of epithelial cells. Deletion of *Spry1/2* in ~80% of the epithelium results in a similar phenotype and disrupts PSG formation, association with the duct, and innervation (Figure S1C).

Epithelial development is important for gangliogenesis

To determine the basis for the loss of parasympathetic gangliogenesis in *Spry1/2DKO* SMGs, we analyzed gangliogenesis between E11.5 (SMG initiation) and E12.5 in wild type embryos. At E11.5 the neural crest-derived TUBB3+ neurons coalesced near the initial epithelial invagination (Figure 2A). However, by E12 a ganglion was closely associated with the epithelial duct and axon bundles began extending towards the single endbud at E12.5 (Figure 2A). These observations suggest that the epithelium may have a role in

ganglia formation. In support of this notion, ganglia did not form in *Fgf10*$^{-/-}$ embryos in which the SMG epithelium does not develop (Ohuchi et al., 2000). Instead we observed dispersed groups of TUBB3+ neuronal cells within and adjacent to the condensed SMG mesenchyme containing an endothelial cell plexus, similar to the neurons in the *Spry1/2DKO* (Figures 2B and 1B). Thus, epithelial development is important for SMG gangliogenesis.

As our results suggested that gangliogenesis is dependent on the epithelium, we hypothesized that secreted signals from the ductal epithelium were critical for ganglia formation. To identify these signals, we performed microarray analysis on isolated primary duct and endbud epithelia at E13 and analyzed genes expressed >5-fold higher in the duct using the Molecular Signatures Database and KEGG Pathways analysis (MSigDB at www.broadinstitute.org). We identified the Wnt pathway as being the most significant signaling pathway enriched in the duct (9 genes; p value of 6.9×10^{-8}). Wnts affect neural crest induction and also neuronal differentiation in the CNS, however their role in parasympathetic gangliogenesis has not been characterized (Dyer et al., 2014; Sauka-Spengler and Bronner-Fraser, 2008; Wexler et al., 2009).

Expression of four Wnts: *Wnt4*, *Wnt5b*, *Wnt7b* and *Wnt10a* were confirmed by qPCR to be enriched in wild-type epithelium as compared to the PSG (Figure 2C) and all four Wnts were more highly expressed in wildtype epithelial duct than the endbuds (Figure 2D). Furthermore, the Wnt receptors frizzled (*Fzd*) 1 and 2, a downstream target of Wnt signaling, *Axin2*, as well as genes previously shown to be involved in SMG parasympathetic function (Knox et al., 2013; Nedvetsky et al., 2014), *Tubb3*, *Vip* and *Chat*, were abundant in the PSG, suggesting secreted Wnts target neurons (Figure 2C).

We next measured Wnt expression levels by qPCR in *Spry1/2DKO* SMGs, in which gangliogenesis does not occur. As expected, there was reduced expression of *Wnt4*, *Wnt7b*, and *Wnt10a* in mutant SMG (40–50%; Figure 2E), although *Wnt5b* expression was not affected, suggesting it may not be important for the mutant phenotype. Expression levels of the FGF ligands *Fgf7* and *Fgf10* were not changed in the *Spry1/2DKO* (Figure 2E). Reduced Wnt signaling was further confirmed by generating *Spry1/2DKO;Axin2*^{Lacz} embryos, where β-galactosidase (βgal) expression and activity marks endogenous Wnt signaling (Haara et al., 2011; Patel et al., 2011). In contrast to control SMGs where βgal staining was within the mesenchyme surrounding the duct, as well as in the distal mesenchyme (Patel et al., 2011), we observed reduced βgal staining adjacent to the SMG epithelial duct of the *Spry1/2DKO;Axin2*^{Lacz} SMGs (Figure S2). In the *Spry1/2DKO* SMGs there was also reduced expression of *Tubb3* (80–90%; Figure 2E) and *Vip* and *Chat* were not detected. In addition, *Krt5* was reduced by 50% (Figure 2E), consistent with the gangliogenesis defect seen in the *Spry1/2DKO* SMGs (Figure 1B and 1C). In contrast, *Krt19* expression was increased, suggesting the K5+ progenitors may be differentiating to K19+ ductal cells, which is consistent with the wide duct phenotype observed in the *Spry1/2DKO* SMGs (Figures 1B and 1E).

Ductal K5+ progenitors produce Wnt signals

Next we determined what epithelial cell type was responsible for producing the Wnt ligands. Given Keratin5-expressing (K5+) progenitor cells are localized to SMG duct in the area most closely associated with ganglia formation and these progenitors are reduced in the *Spry1/2DKO* along with Wnts, we predicted that K5+ cells were the source of Wnt ligands. To test this prediction, we FACS-sorted K5+ and K5- epithelial cells from E13 *K5-Venus*-expressing SMGs (Knox et al., 2010). The K5+ cells comprise ~14.9 percent of the SMG epithelial cells. qPCR analysis of *Wnt* expression in the sorted cells confirmed that expression of the four *Wnts* identified in our screen were enriched in K5+ compared to K5- epithelial cells: *Wnt4* (3.6-fold), *Wnt5b* (1.8-fold), *Wnt7b* (18.1-fold), and *Wnt10a* (11.8-fold) (Figure 2F). These data identify the K5+ progenitors within the duct as the major source of these Wnt ligands.

Wnt signaling promotes neuronal proliferation and survival in the PSG

Since Wnts are produced by the duct epithelium we next tested the functional response of parasympathetic neuronal cells to Wnt ligands. First, we confirmed that Wnt signaling occurs in the PSG by analyzing the PSG in $Axin2^{LacZ}$ Wnt-reporter mice. Active WNT signaling in mesenchymal cells adjacent to the SMG duct and in the cap mesenchyme had been previously reported (Patel et al., 2011). We found βgal expression localized to the neuronal cell bodies of the PSG (Figure 3A), consistent with our hypothesis that active Wnt signaling occurs within PSG neurons. We also confirmed that the developing PSG neurons are not post-mitotic and are still proliferating in response to endogenous signals in vivo up to E14 (Figure 3B). To directly test the response of parasympathetic neuronal cells to Wnt signaling we measured changes in proliferation and cell death in isolated E12 PSGs treated with recombinant Wnt4, one of the Wnt ligands expressed by K5+ progenitors in the duct (Figures 3C and 3D). Wnt4 treatment of either intact E12 SMGs or isolated PSGs in culture increased neuronal cell proliferation ~3 fold as measured by the number of PH3+ neurons (Figures 3C and S3). Wnt4 also reduced neuronal cell death in isolated PSG cultures by ~35% compared to BSA-treated controls (Figure 3D). Thus Wnt signaling promotes both PSG neuronal cell survival and proliferation.

Wnt expression is negatively regulated by MAPK-dependent FGF signaling and positively regulated by PI3K-dependent neuregulin signaling

Our results from the *Spry1/2DKO* SMGs suggest that increasing FGF signaling antagonizes Wnt transcription and activity, similar to findings in other organs (Mansukhani et al., 2005; Minor et al., 2013). To investigate the mechanisms by which FGF signaling antagonizes Wnt activity we first treated E12 $Axin2^{LacZ}$ SMGs with FGFs and confirmed that Wnt signaling decreased within 24 h as shown by reduced βgal staining (Figure 4A). We then used shorter times of FGF treatment (1, 2, 6 as well as 24 h) and analyzed the timing of the reduction in Wnt expression (Figure 4B). Treatment of E12 SMGs with FGFs reduced expression of *Wnt4*, *Wnt7b and Wnt10a* (~30–50%) within 6 h (Figure 4B), whereas *Wnt5b* expression was not significantly affected, similar to the *Spry1/2DKO* (Figure 2E). There was ~50% reduction in *Axin2* and *Krt5* transcripts by 24 h. In contrast, *Krt19* expression increased suggesting Krt5+ cells were differentiating, similar to the *Spry1/2DKO*. There was

also increased expression of *Spry1* and *Spry2*, which are induced by FGF signaling. Together, these data show that excess FGF signaling in E12 SMG cultures mimics the in vivo deletion of Spry1 and Spry2 and that FGF signaling rapidly reduces the expression of the cohort of Wnts produced by the K5+ progenitors.

To further investigate the mechanisms by which FGF signaling regulates Wnt expression and to identify the downstream signaling pathways involved, we used isolated epithelia devoid of mesenchyme and PSG. Isolated epithelia were treated for 4 h with FGF10 (which allows the isolated epithelia to survive in culture) and either an FGFR2b inhibitor (Fgfr2b-Fc, 25 nM), a mitogen-activated protein kinase (MAPK) inhibitor (U0126, 20 μM), a phosphatidylinositol 3-kinase (PI3K) inhibitor (LY294002, 25 μM), or an epidermal growth factor receptor (EGFR) inhibitor (PD168393, 10 μM), which also inhibits other erbB receptors (Figure 4C). As predicted, inhibiting FGFR2b or MAPK signaling in the SMG epithelia increased *Wnt4*, *Wnt5b* and *Wnt10a* expression 3–6 fold within 4 h (Figure 4C). Interestingly, inhibition of EGFR or PI3K decreased *Wnt4*, *Wnt5b*, *Wnt7b* and *Wnt10a* suggesting that Wnt expression is positively regulated by PI3K downstream of erbB signaling (Figure 4C). To investigate the erbB regulation of Wnt expression in the epithelium, isolated epithelia were treated with FGF10, and three erbB ligands that are involved in SMG epithelial development (Kera et al., 2014; Miyazaki et al., 2004). Addition of HBEGF, Tgfα or Nrg1 alone shows that that they rapidly increase *Wnt4*, *Wnt5b* and *Wnt10a* expression within 4 h (Figure 4D). Since Nrg1 had the greatest inductive affect on Wnt expression we confirmed that Wnt expression was dependent on PI3K signaling by co-incubating the isolated epithelia with the erbB inhibitor (PD) and PI3K inhibitor (LY) for 2 h along with Nrg1 (Figure 4E). Both PD and LY reduced the expression of *Wnt4*, *Wnt5b*, *Wnt7b* and *Wnt10a* that was induced by Nrg1. LY also reduced the expression of *Wnt5b*, *Wnt7b* and *Wnt10a* below that in untreated epithelia. We confirmed by FACs analysis that the K5+ cells in E12 epithelia also expressed the erbB receptors *Egfr*, *Erbb2* and *Erbb3* (Figure 4F). To determine if erbB signaling components were affected in the *Spry1/2DKO* we analyzed E13 SMGs by qPCR, however we did not detect any changes in *Nrg1*, *Erbb2* or *Erbb3* expression (Figure S4). Taken together, our data shows that MAPK-dependent FGF signaling represses Wnt expression whereas PI3K-dependent erbB signaling upregulates it in salivary epithelium.

Inhibition of Wnt signaling disrupts gangliogenesis and ganglion function

To assess the effects of reducing Wnt signaling on gangliogenesis we used ex vivo E11 mandible slice culture, which recapitulates SMG initiation and gangliogenesis ex vivo. The mandible slices contain the developing tongue, associated oral epithelium and mesenchyme. Within 48 h of culture the SMG epithelium initiates within a condensed mesenchyme to form a duct and endbud and gangliogenesis occurs, with subsequent axon extension towards the endbuds (Figure 5A–C). Treatment with either of two different Wnt signaling inhibitors, Dkk1 or XAV939, during SMG initiation did not perturb the initial epithelial morphogenesis or duct elongation, however gangliogenesis appeared disrupted as multiple small clusters of neurons were observed within the mesenchyme (Figures 5B and S5). We also measured the area of the PSG overlying the duct, axon number, and epithelial endbud number (Figure 5C). By analyzing a projection of the nerve and epithelial immunostaining we show that in

control SMGs, ~46% of the PSG area overlays the duct, and with Wnt inhibitor treatment only 20–30% of the PSG area overlays the duct (Figure 5C). Quantitation of the number of axons contacting the epithelial buds and the number of end buds shows a reduction in both axon and end bud number with XAV939 treatment and a similar, but not significant, trend with Dkk1 treatment (Figure 5B and 5C). We also downregulated endogenous Wnt expression with FGF stimulation, which mimics the *Spry1/2DKO* (see Figure S2). Treatment with exogenous FGFs (both Fgf7 and Fgf10) during SMG initiation results in a slight, but not significant increase in endbud number and a striking loss of primary duct formation, most likely due to a disruption of the discrete localization of FGF required to establish a signaling gradient that is critical for duct elongation (Makarenkova et al., 2009). FGF stimulation also reduced the area of the PSG overlying the duct and the axon number (Figures 5B, 5C and S5).

To determine whether Wnt signaling is also required to maintain association of the PSG with the epithelium and PSG-maintenance of progenitor cells, we treated intact E12.5 SMGs with FGFs (Figure 5D). After 48 h of FGF treatment, the PSG no longer associated with the epithelium and fewer axons extended from the ganglion towards the endbuds (Figure 5D). In addition, ectopic buds formed on the duct, which was wider than the duct in the control SMG (Figure 5D). Concomitant with this reduced innervation was a reduction in K5+ progenitors within the duct, whereas there was an expansion of K19 staining, a marker of ductal differentiation (Figure 5D). Collectively, these results indicate that Wnt signaling is required for gangliogenesis and to sustain the association of the PSG with the duct, which increases epithelial innervation and subsequent maintenance of undifferentiated K5+ progenitors.

Reducing FGF gene dosage rescues duct formation in vivo

Based on these results, we predicted that reducing FGF gene dosage in *Spry1/2DKO* embryos would lower FGF signaling, rescue duct formation, and restore gangliogenesis. However, removing a single copy of *Fgf7* and/or *Fgf10* in the *Spry1/2DKO* (*Spry1/2DKO;Fgf7*$^{+/-}$, *Spry1/2DKO;Fgf10*$^{+/-}$, or *Spry1/2DKO;Fgf7*$^{+/-}$*;Fgf10*$^{+/-}$) did not rescue parasympathetic gangliogenesis and innervation, although duct formation was rescued in *Spry1/2DKO;Fgf7*$^{+/-}$*;Fgf10*$^{+/-}$ SMGs (Figure S6A and S6B). These data suggest that FGF signaling within the epithelium is critical for duct formation, which is consistent with the ability of isolated salivary epithelial explants to form ducts in the absence of PSG in vitro. These data also suggested that there was still insufficient Wnt activation to restore gangliogenesis.

Increasing Wnt signaling while decreasing FGF gene dosage rescues gangliogenesis in vivo

We then predicted that in addition to reducing FGF gene dosage in *Spry1/2DKO* embryos we needed to activate Wnt signaling in utero, which would rescue gangliogenesis and K5+ progenitor cells. To test this prediction, we treated pregnant mice with a Wnt activator (CT99021) to target the *Spry1/2DKO* embryos. Gangliogenesis and innervation were not improved when *Spry1/2DKO* embryos were treated with a single in utero dose of the Wnt activator alone (Figure 6A and 6B). However, using the Wnt activator in combination with

removal of a single copy of *Fgf10* to lower FGF signaling (*Spry1/2DKO;Fgf10*$^{+/-}$) rescued gangliogenesis, innervation and duct development (Figures 6A–C). Endbud number, the relative size of the PSG and the relative number of axons (normalized to epithelial area) were increased in the *Spry1/2DKO;Fgf10*$^{+/-}$ SMGs treated with Wnt activator as compared to both untreated and Wnt activator-treated *Spry1/2DKO* SMGs (Figure 6C). Consistent with this rescued innervation, K5+ progenitors were present in the ducts of SMGs from *Spry1/2DKO;Fgf10*$^{+/-}$ embryos treated with Wnt activator (Figures 6D and 6E). Addition of the Wnt activator was essential since gene expression analysis of "rescued" *Spry1/2DKO;Fgf10*$^{+/-}$ embryos treated with Wnt activator revealed *Fgf10* was reduced, as expected since a copy of *Fgf10* was deleted. Expression of the neuronal genes *Vip* and *Chat* increased, although not completely to control levels (Figure 6E). CT99021 treatment increased *Vip* expression to detectable levels in 3/4 *Spry1/2DKO* mutant SMGs and 5/6 *Spry1/2DKO;Fgf10*$^{+/-}$ SMGs. *Chat* was not detected in any of the *Spry1/2DKO* mutant SMGs but was increased in 4/6 *Spry1/2DKO;Fgf10*$^{+/-}$ SMGs (Figure 6E). *Axin2* expression was slightly but not significantly reduced in mutant and rescued glands, which may be due to the relative increase in FGFR signaling, similar to that shown in Figure 4B. Importantly, *Wnt4*, *Wnt7b*, *Wnt10a* and *Krt5* expression increased to, or near, control levels in the rescued SMGs (Figure 6E).

Parasympathetic ganglia innervate multiple organs during development. Therefore, we tested whether Sprouty-dependent Wnt signaling controls gangliogenesis in other organs such as the developing pancreas. In the pancreas, parasympathetic nerves control pancreatic β-cell regeneration (Medina et al., 2013), GDNF signaling is required for neural colonization in fetal pancreas (Munoz-Bravo et al., 2013) and deletion of GDNF family members, or the co-receptor *Ret*, cause deficits in multiple parasympathetic ganglia (Enomoto et al., 2000; Rossi and Airaksinen, 2002). In the wild-type E14 mouse pancreas multiple small clusters of intrapancreatic ganglia expressing the parasympathetic neuronal marker GFRα2 are interspersed throughout the tissue (Figure 6F). Similar to the SMG, deletion of *Spry1/2* resulted in a dramatic reduction in pancreatic parasympathetic ganglia, suggesting that Sprouty-dependent Wnt signaling pathways also control parasympathetic gangliogenesis and innervation in the pancreas (Figure 6F). Removing one copy of *Fgf10* in combination with treatment with the Wnt activator (CT99021) also rescued pancreas gangliogenesis in vivo (Figure 6F). Taken together, these data show that Spry1/2-dependent Wnt signals are key regulators of parasympathetic gangliogenesis during epithelial organ development.

DISCUSSION

Previous studies have shown that regulation of FGF signaling is necessary for the establishment of cranial nerves. However the signals regulating gangliogenesis are not well understood (Steventon et al., 2014). Here we show that Wnt signals from the epithelium are necessary for formation of the PSG and that this activity is antagonized by FGF signaling. Importantly, we identify K5+ progenitor cells as the source of Wnt signals that promote parasympathetic neuronal survival and proliferation, PSG formation and gland innervation. Lastly, we demonstrate that the production of Wnt ligands is inhibited by FGFR2b/MAPK signaling and promoted through an erbB/PI3K dependent pathway. As such we provide a

mechanism by which an organ and more specifically progenitor cells regulate their own innervation that is required for organogenesis (Figure 7).

Wnt signaling plays a key role in neural development and patterning of both the central and peripheral nervous systems (Mulligan and Cheyette, 2012). Based on our observation that reducing epithelial Wnt signals impairs gangliogenesis, we speculate that neuronal-neuronal cell interactions within the PSG are also dependent on Wnt signaling. Wnt signaling can increase cell-cell adhesion through the induction of molecules such as L1CAM and NCAM (Gavert et al., 2005; Piloto and Schilling, 2010). Furthermore, mutations in NRG1, which we show increases WNT expression, L1CAM and integrin beta1 occur in patients with aganglionic megacolon or Hirschsprung's disease also suggest this to be a mechanism of regulating gangliogenesis (Bergeron et al., 2013). Our findings highlight the importance of bi-directional epithelial-neuronal communication; reducing epithelial Wnt expression decreases mesenchymal Wnt signaling and impairs gangliogenesis, leading to depletion of epithelial K5+ progenitors, which are essential for gland morphogenesis.

Our study reveals an interaction between the epithelium and coalescing neurons that is necessary for gangliogenesis. Unlike for sensory gangliogenesis, where reciprocal signaling between the neural crest cells and cranial placode cells is required for gangliogenesis (Simoes-Costa and Bronner, 2013; Steventon et al., 2014), we identify an essential role for the epithelium in coordinating ganglia formation. However, it remains to be determined if some of the other signaling systems that guide sensory gangliogenesis also occur during formation of the parasympathetic ganglia. For example, sensory gangliogenesis involves Robo2 expressed by placode cells and its ligand Slit1 expressed by the neural crest (Shiau et al., 2008). Robo2-Slit1 signaling between neural crest and placode cells affects the cellular localization N-cadherin to promote gangliogenesis (Shiau and Bronner-Fraser, 2009). Whether this also occurs in parasympathetic gangliogenesis remains to be explored.

Our finding that K5+ progenitor cells promote their own innervation is similar to the KIT+ progenitor cells, another progenitor population in SMG epithelial endbuds, which produce neurturin to maintain parasympathetic innervation (Lombaert et al., 2013). These findings highlight the importance of bi-directional neuronal-epithelial communication during organogenesis. As such, the progenitors themselves establish a vital component of the stem cell niche during organ formation.

Sproutys play a key role in restricting FGF signaling to allow for proper development of a number of organs, including the inner ear, lung and spleen (Chai et al., 2000; Shim et al., 2005; Tang et al., 2011). When Sproutys are deleted cell differentiation and/or organ morphogenesis are perturbed, such as in the inner ear where loss of *Spry2* results in a cell fate change that disrupts the cytoarchitecture of the organ of Corti. FGF signaling is normally required for salivary gland organogenesis (Figure 2B), promoting cell proliferation in the endbuds to drive branching morphogenesis (Entesarian et al., 2005; Steinberg et al., 2005). We find that too much FGF signaling derails normal SMG development in part by inhibiting gangliogenesis through loss of Wnt expression by K5+ progenitors and in turn causes abnormal ductal differentiation, depletion of progenitors and aberrant morphogenesis (Figures 1 and 2). Moreover, we show that ErbB signaling regulates ductal cells by inducing

Wnt expression in the epithelia, suggesting deletion of Sprouty 1 and 2 upsets the balance of FGF and ErbB3 signaling. Perturbation of erbB signaling by either deletion of EGFR in vivo (Haara et al., 2009) or antibody inhibition of HBEGF and Nrg1 in culture reduces SMG branching (Miyazaki et al., 2004; Umeda et al., 2001). Additionally, ductal differentiation occurs in the absence of ganglia by autocrine HBEGF/erbB signaling in the epithelium (Knox et al., 2010). However, in previous reports on erbB function Wnt signaling was not analyzed. Our data suggest that the balance of FGF/erbB signaling regulates Wnt expression and Wnt ligands act on neuronal cells to promote survival and proliferation. Given survival and proliferation of the Schwann cell precursors that form the PSG were shown to require Nrg1/ErbB signaling (Dyachuk et al., 2014), Wnt signals may also be involved in earlier steps of gangliogenesis. Future studies are needed to determine the involvement of the different erbB receptors and their ligands, as well as the balance of FGF and Wnt signaling pathways in the development of epithelial-neuronal communication. In addition, we cannot rule out the possibility that developing endothelial cells may provide FGF, Wnt and/or erbB signals to both neuronal and epithelial cells during SMG development.

In summary, we have defined an essential role for Spry1/2-dependent Wnt signaling in neuronal survival, proliferation and parasympathetic gangliogenesis. Importantly, we also find that a similar mechanism occurs in the pancreas. Further studies exploring the innervation of the pancreas are required and may have implications for type-2 diabetes where there is already a connection between Wnt signaling and glucose metabolism (Li et al., 2012). We suggest that localized manipulation of Wnt signals may provide a mechanism to promote gangliogenesis and improve organ innervation for repair or regeneration of salivary glands, the pancreas or in the colon such as in Hirschsrpung's disease.

MATERIALS AND METHODS

Mouse strains and gavage

Mice carrying *ACTB-cre* (Lewandoski and Martin, 1997), $Wnt1^{cre}$ (Danielian et al., 1998), *Spry1* null and $Spry1^{flox}$ (Tang et al., 2011), *Spry2* null (Shim et al., 2005), $Spry2^{flox}$ (Shim et al., 2005), *Fgf7* null (Guo et al., 1996), *Fgf10* null (Min et al., 1998), *K5-Venus* (Knox et al., 2010), and $Axin2^{lacZ}$ (Lustig et al., 2002) alleles have been previously described. $Spry1^{-/-}$;$Spry2^{-/-}$ double knockout embryos (*Spry1/2DKO*) were generated by crossing *ACTB-cre*;$Spry1^{+/-}$;$Spry2^{+/-}$ males to $Spry1^{fl/fl}$;$Spry2^{fl/fl}$ females as previously described (Tang et al., 2011). Wild-type embryos were obtained from ICR timed pregnant females (Harlan). To generate the embryos used in this study, timed matings were performed and the morning of the day a plug was detected was considered Day 0. The Wnt activator CT99021 (#S2924, Selleckchem) was administered by oral gavage to timed pregnant females on day 10 after detection of a plug as a single 200 μl dose per pregnant female at a concentration of 1 mg/mL in sunflower oil.

Immunostaining, imaging and fluorescence quantitation

All tissues were processed and imaged as whole mount specimens unless otherwise noted. Tissues were blocked and immunostained as previously described (Steinberg et al., 2005), with the modification that primary antibodies were incubated overnight at 4°C. Antibodies

are listed in the Supplemental Experimental Procedures. Imaging was performed using a Zeiss LSM 710 confocal microscope system. Z stack images were processed using NIH/ImageJ or Volocity (Perkin Elmer). PSG area, epithelial area and number of axons were determined using ImageJ. The percentage of PSG area overlying the duct was calculated by dividing the PSG area over the duct by the total PSG area.

Ex vivo cultures

E12.5 PSGs were isolated and cultured for 24 hours as previously described (Knox et al., 2013). Mandibles were dissected from E11 embryos by isolating the lower mandible and mechanically removing the tissue surrounding the tongue and oral epithelium with fine forceps. Mandibles and SMGs were cultured in serum-free media at 37°C as previously described (Knox et al., 2010). A list of the proteins and chemicals used are provided in the Supplementary Experimental Procedures.

Microarray analysis

Agilent microarray analysis (Agilent, CA) was performed as described by the manufacturers instructions. The array data is from the SGMAP Database (Salivary Gland Molecular Anatomy Project, http://sgmap.nidcr.nih.gov/sgmap/sgexp.html).

XGAL staining

XGAL staining was performed as previously described (Patel et al., 2011). A detailed protocol is provided in the Supplementary Experimental Procedures.

Quantitative PCR

RNA was isolated using an RNAqueous-Micro kit with DNase treatment (Ambion). cDNA was synthesized using the iScript cDNA Synthesis Kit (Biorad). For real-time PCR 1 ng of each cDNA was amplified with 40 cycles of 95°C for 10 seconds and 62°C for 30 seconds. Gene expression was normalized to the housekeeping gene, *Rps29*. We also used TaqMan low-density arrays where gene expression was normalized to *Rps18*. Amplification of a single product was confirmed by melt curve analysis and all reactions were run in triplicate. Data were log transformed before all statistical analyses. Prism 6 software (GraphPad) was used to perform one-way ANOVA with post hoc Dunnett's test to compare more than two experimental groups. For comparison of two data sets the Student's t-test was used to calculate P values in Microsoft excel, with two-tailed tests and unequal variance. Graphs show the mean +/− SEM for each group from three or more experiments unless otherwise noted.

Fluorescence-activated cell sorting analysis

E12-E13 SMGs from *K5-venus* embryos were dissociated as previously described (Mulligan and Cheyette, 2012). Single cell suspensions were incubated with a fluorescent-labeled CD326 antibody (BD Biosciences), sorted based on CD326 and Venus expression on a BD FACSAria, and processed for RNA isolation and qPCR as described above. Data were normalized to *Rps29* and fold change was calculated as K5+ cell expression level compared to K5- cell expression level for each gene.

Supplementary Material

Refer to Web version on PubMed Central for supplementary material.

Acknowledgments

The authors would like to thank Dr. Gail R. Martin, in whose laboratory at UCSF this collaboration started, for providing critical input into the design, experimental details and for sharing many of the mouse strains used; Prajakta Ghatpande and Elsa Berenstein for technical assistance and maintenance of the mouse colonies required for these studies; Joao Ferreira, Ryan Petrie and Kelly Ten Hagen for critical reading of the manuscript. This research was supported by the Intramural Research Program of the National Institute of Dental and Craniofacial Research at the National Institutes of Health.

References

Bergeron KF, Silversides DW, Pilon N. The developmental genetics of Hirschsprung's disease. Clin Genet. 2013; 83:15–22. [PubMed: 23043324]

Chai Y, Jiang X, Ito Y, Bringas P Jr, Han J, Rowitch DH, Soriano P, McMahon AP, Sucov HM. Fate of the mammalian cranial neural crest during tooth and mandibular morphogenesis. Development. 2000; 127:1671–1679. [PubMed: 10725243]

Coughlin MD. Early development of parasympathetic nerves in the mouse submandibular gland. Developmental biology. 1975; 43:123–139. [PubMed: 1149921]

Danielian PS, Muccino D, Rowitch DH, Michael SK, McMahon AP. Modification of gene activity in mouse embryos in utero by a tamoxifen-inducible form of Cre recombinase. Curr Biol. 1998; 8:1323–1326. [PubMed: 9843687]

De Moerlooze L, Spencer-Dene B, Revest JM, Hajihosseini M, Rosewell I, Dickson C. An important role for the IIIb isoform of fibroblast growth factor receptor 2 (FGFR2) in mesenchymal-epithelial signalling during mouse organogenesis. Development. 2000; 127:483–492. [PubMed: 10631169]

Dyachuk V, Furlan A, Shahidi MK, Giovenco M, Kaukua N, Konstantinidou C, Pachnis V, Memic F, Marklund U, Muller T, et al. Neurodevelopment. Parasympathetic neurons originate from nerve-associated peripheral glial progenitors. Science. 2014; 345:82–87. [PubMed: 24925909]

Dyer C, Blanc E, Hanisch A, Roehl H, Otto GW, Yu T, Basson MA, Knight R. A bi-modal function of Wnt signalling directs an FGF activity gradient to spatially regulate neuronal differentiation in the midbrain. Development. 2014; 141:63–72. [PubMed: 24284206]

Enomoto H, Heuckeroth RO, Golden JP, Johnson EM, Milbrandt J. Development of cranial parasympathetic ganglia requires sequential actions of GDNF and neurturin. Development. 2000; 127:4877–4889. [PubMed: 11044402]

Entesarian M, Matsson H, Klar J, Bergendal B, Olson L, Arakaki R, Hayashi Y, Ohuchi H, Falahat B, Bolstad AI, et al. Mutations in the gene encoding fibroblast growth factor 10 are associated with aplasia of lacrimal and salivary glands. Nat Genet. 2005; 37:125–127. [PubMed: 15654336]

Espinosa-Medina I, Outin E, Picard CA, Chettouh Z, Dymecki S, Consalez GG, Coppola E, Brunet JF. Neurodevelopment. Parasympathetic ganglia derive from Schwann cell precursors. Science. 2014; 345:87–90. [PubMed: 24925912]

Gavert N, Conacci-Sorrell M, Gast D, Schneider A, Altevogt P, Brabletz T, Ben-Ze'ev A. L1, a novel target of beta-catenin signaling, transforms cells and is expressed at the invasive front of colon cancers. J Cell Biol. 2005; 168:633–642. [PubMed: 15716380]

Guo L, Degenstein L, Fuchs E. Keratinocyte growth factor is required for hair development but not for wound healing. Genes Dev. 1996; 10:165–175. [PubMed: 8566750]

Haara O, Fujimori S, Schmidt-Ullrich R, Hartmann C, Thesleff I, Mikkola ML. Ectodysplasin and Wnt pathways are required for salivary gland branching morphogenesis. Development. 2011; 138:2681–2691. [PubMed: 21652647]

Haara O, Koivisto T, Miettinen PJ. EGF-receptor regulates salivary gland branching morphogenesis by supporting proliferation and maturation of epithelial cells and survival of mesenchymal cells. Differentiation; research in biological diversity. 2009; 77:298–306.

Kera H, Yuki S, Nogawa H. FGF7 signals are relayed to autocrine EGF family growth factors to induce branching morphogenesis of mouse salivary epithelium. Dev Dyn. 2014; 243:552–559. [PubMed: 24227310]

Knosp WM, Knox SM, Hoffman MP. Salivary gland organogenesis. Wiley interdisciplinary reviews. Developmental biology. 2012; 1:69–82. [PubMed: 23801668]

Knox SM, Lombaert IM, Haddox CL, Abrams SR, Cotrim A, Wilson AJ, Hoffman MP. Parasympathetic stimulation improves epithelial organ regeneration. Nat Commun. 2013; 4:1494. [PubMed: 23422662]

Knox SM, Lombaert IMA, Reed X, Vitale-Cross L, Gutkind JS, Hoffman MP. Parasympathetic innervation maintains epithelial progenitor cells during salivary organogenesis. Science. 2010; 329:1645–1647. [PubMed: 20929848]

Lewandoski M, Martin GR. Cre-mediated chromosome loss in mice. Nature genetics. 1997; 17:223–225. [PubMed: 9326948]

Li X, Shan J, Chang W, Kim I, Bao J, Lee HJ, Zhang X, Samuel VT, Shulman GI, Liu D, et al. Chemical and genetic evidence for the involvement of Wnt antagonist Dickkopf2 in regulation of glucose metabolism. Proc Natl Acad Sci U S A. 2012; 109:11402–11407. [PubMed: 22733757]

Lombaert IM, Abrams SR, Li L, Eswarakumar VP, Sethi AJ, Witt RL, Hoffman MP. Combined KIT and FGFR2b signaling regulates epithelial progenitor expansion during organogenesis. Stem Cell Reports. 2013; 1:604–619. [PubMed: 24371813]

Lustig B, Jerchow B, Sachs M, Weiler S, Pietsch T, Karsten U, van de Wetering M, Clevers H, Schlag PM, Birchmeier W, et al. Negative feedback loop of Wnt signaling through upregulation of conductin/axin2 in colorectal and liver tumors. Mol Cell Biol. 2002; 22:1184–1193. [PubMed: 11809809]

Makarenkova HP, Hoffman MP, Beenken A, Eliseenkova AV, Meech R, Tsau C, Patel VN, Lang RA, Mohammadi M. Differential interactions of FGFs with heparan sulfate control gradient formation and branching morphogenesis. Sci Signal. 2009; 2:ra55. [PubMed: 19755711]

Mansukhani A, Ambrosetti D, Holmes G, Cornivelli L, Basilico C. Sox2 induction by FGF and FGFR2 activating mutations inhibits Wnt signaling and osteoblast differentiation. J Cell Biol. 2005; 168:1065–1076. [PubMed: 15781477]

Medina A, Yamada S, Hara A, Hamamoto K, Kojima I. Involvement of the parasympathetic nervous system in the initiation of regeneration of pancreatic beta-cells. Endocrine journal. 2013; 60:687–696. [PubMed: 23411584]

Milunsky JM, Zhao G, Maher TA, Colby R, Everman DB. LADD syndrome is caused by FGF10 mutations. Clin Genet. 2006; 69:349–354. [PubMed: 16630169]

Min H, Danilenko DM, Scully SA, Bolon B, Ring BD, Tarpley JE, DeRose M, Simonet WS. Fgf-10 is required for both limb and lung development and exhibits striking functional similarity to Drosophila branchless. Genes Dev. 1998; 12:3156–3161. [PubMed: 9784490]

Minor PJ, He TF, Sohn CH, Asthagiri AR, Sternberg PW. FGF signaling regulates Wnt ligand expression to control vulval cell lineage polarity in C. elegans. Development. 2013; 140:3882–3891. [PubMed: 23946444]

Minowada G, Jarvis LA, Chi CL, Neubuser A, Sun X, Hacohen N, Krasnow MA, Martin GR. Vertebrate Sprouty genes are induced by FGF signaling and can cause chondrodysplasia when overexpressed. Development. 1999; 126:4465–4475. [PubMed: 10498682]

Miyazaki Y, Nakanishi Y, Hieda Y. Tissue interaction mediated by neuregulin-1 and ErbB receptors regulates epithelial morphogenesis of mouse embryonic submandibular gland. Dev Dyn. 2004; 230:591–596. [PubMed: 15254894]

Mulligan KA, Cheyette BN. Wnt signaling in vertebrate neural development and function. J Neuroimmune Pharmacol. 2012; 7:774–787. [PubMed: 23015196]

Munoz-Bravo JL, Hidalgo-Figueroa M, Pascual A, Lopez-Barneo J, Leal-Cerro A, Cano DA. GDNF is required for neural colonization of the pancreas. Development. 2013; 140:3669–3679. [PubMed: 23903190]

Nedvetsky PI, Emmerson E, Finley JK, Ettinger A, Cruz-Pacheco N, Prochazka J, Haddox CL, Northrup E, Hodges C, Mostov KE, et al. Parasympathetic innervation regulates tubulogenesis in the developing salivary gland. Dev Cell. 2014; 30:449–462. [PubMed: 25158854]

Ohuchi H, Hori Y, Yamasaki M, Harada H, Sekine K, Kato S, Itoh N. FGF10 acts as a major ligand for FGF receptor 2 IIIb in mouse multi-organ development. Biochem Biophys Res Commun. 2000; 277:643–649. [PubMed: 11062007]

Patel N, Sharpe PT, Miletich I. Coordination of epithelial branching and salivary gland lumen formation by Wnt and FGF signals. Developmental biology. 2011; 358:156–167. [PubMed: 21806977]

Piloto S, Schilling TF. Ovo1 links Wnt signaling with N-cadherin localization during neural crest migration. Development. 2010; 137:1981–1990. [PubMed: 20463035]

Rossi J, Airaksinen MS. GDNF family signalling in exocrine tissues: distinct roles for GDNF and neurturin in parasympathetic neuron development. Advances in experimental medicine and biology. 2002; 506:19–26. [PubMed: 12613884]

Sauka-Spengler T, Bronner-Fraser M. A gene regulatory network orchestrates neural crest formation. Nat Rev Mol Cell Biol. 2008; 9:557–568. [PubMed: 18523435]

Shiau CE, Bronner-Fraser M. N-cadherin acts in concert with Slit1-Robo2 signaling in regulating aggregation of placode-derived cranial sensory neurons. Development. 2009; 136:4155–4164. [PubMed: 19934013]

Shiau CE, Lwigale PY, Das RM, Wilson SA, Bronner-Fraser M. Robo2-Slit1 dependent cell-cell interactions mediate assembly of the trigeminal ganglion. Nat Neurosci. 2008; 11:269–276. [PubMed: 18278043]

Shim K, Minowada G, Coling DE, Martin GR. Sprouty2, a mouse deafness gene, regulates cell fate decisions in the auditory sensory epithelium by antagonizing FGF signaling. Dev Cell. 2005; 8:553–564. [PubMed: 15809037]

Simoes-Costa M, Bronner ME. Insights into neural crest development and evolution from genomic analysis. Genome research. 2013; 23:1069–1080. [PubMed: 23817048]

Simrick S, Lickert H, Basson MA. Sprouty genes are essential for the normal development of epibranchial ganglia in the mouse embryo. Developmental biology. 2011; 358:147–155. [PubMed: 21806979]

Steinberg Z, Myers C, Heim VM, Lathrop CA, Rebustini IT, Stewart JS, Larsen M, Hoffman MP. FGFR2b signaling regulates ex vivo submandibular gland epithelial cell proliferation and branching morphogenesis. Development. 2005; 132:1223–1234. [PubMed: 15716343]

Steventon B, Mayor R, Streit A. Neural crest and placode interaction during the development of the cranial sensory system. Developmental biology. 2014; 389:28–38. [PubMed: 24491819]

Tang N, Marshall WF, McMahon M, Metzger RJ, Martin GR. Control of mitotic spindle angle by the RAS-regulated ERK1/2 pathway determines lung tube shape. Science. 2011; 333:342–345. [PubMed: 21764747]

Umeda Y, Miyazaki Y, Shiinoki H, Higashiyama S, Nakanishi Y, Hieda Y. Involvement of heparin-binding EGF-like growth factor and its processing by metalloproteinases in early epithelial morphogenesis of the submandibular gland. Developmental biology. 2001; 237:202–211. [PubMed: 11518516]

Wexler EM, Paucer A, Kornblum HI, Palmer TD, Geschwind DH. Endogenous Wnt signaling maintains neural progenitor cell potency. Stem Cells. 2009; 27:1130–1141. [PubMed: 19418460]

Yu T, Yaguchi Y, Echevarria D, Martinez S, Basson MA. Sprouty genes prevent excessive FGF signalling in multiple cell types throughout development of the cerebellum. Development. 2011; 138:2957–2968. [PubMed: 21693512]

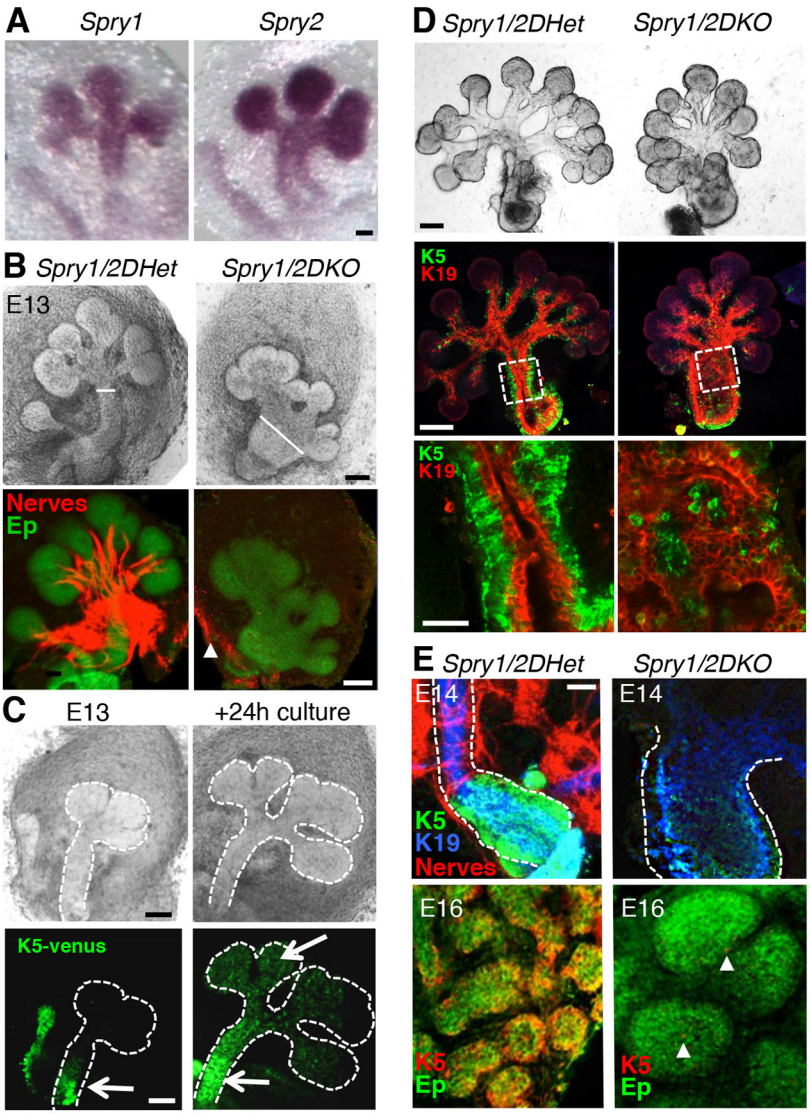

Figure 1. Spry1/2 are required for parasympathetic gangliogenesis, organ innervation and K5+ progenitor cell maintenance

(A) In situ hybridization of wild-type E13 SMGs. Scale bar, 50 μm. (B) E14 *Spry1/2DHet* and *Spry1/2DKO* SMGs, brightfield images and immunostaining for indicated markers, *n* = 52. Scale bar, 100 μm. (C) K5+ cells are in the epithelial duct (green, white arrow) in E13 K5-venus SMGs. After 24 h of culture K5+ cells are in the ducts and endbuds (white arrows). Scale bars, 100 μm. (D) *Spry1/2DHet* and *Spry1/2DKO* epithelia cultured for 72 h and immunostained for K5 and K19. Scale bar, 25 μm. White boxes are shown at high power below. Scale bar, 50 μm. *n* = 4. (E) Immunostaining of E14 and E16 *Spry1/2DHet* and *Spry1/2DKO* SMGs. E14 ducts immunostained for K5, K19 and nerves (Tubb3). E16 endbuds immunostained for K5 (red) and epithelium (Ep, E-cadherin). White arrowhead points to K5 cells in the *Spry1/2DKO*. *n* = 3. Scale bar, 100 μm. See also Figure S1 and Supplementary Table 1.

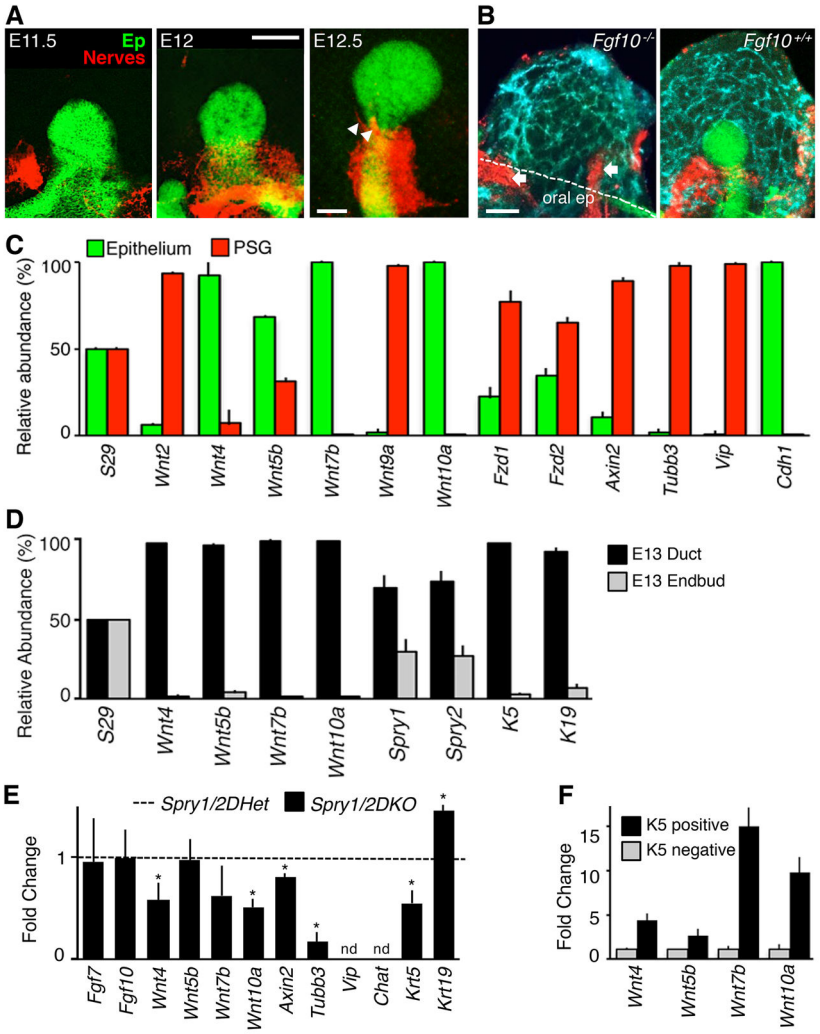

Figure 2. Ductal K5+ progenitor cells express Wnt ligands

(A) Immunostaining of E11.5–12.5 wild-type SMGs for epithelium (Ep, E-cadherin) and nerves (Tubb3). Arrowheads indicate axonal projections. Scale bar, 100 μm. (B) Immunostaining of *Fgf10*$^{-/-}$ and *Fgf10*$^{+/+}$ SMGs for epithelium, nerves and endothelium (PECAM), $n = 10$. White dotted lines outline the oral epithelium (oral ep); arrows indicate nerves in the adjacent tongue and oral epithelium. Scale bar, 50 μm. (C) qPCR analysis of E12 epithelium and PSG, graphed as a percentage of relative abundance, $n = 3$. (D) qPCR analysis of E13 epithelial ducts and endbuds, graphed as a percentage of relative abundance, $n = 3$. (E) qPCR analysis of E13 *Spry1/2DKO* SMGs compared to *Spry1/2DHet*. $n = 4$. Note, 1 out of 4 mutant samples had a low level of Vip and Chat expression; the other 3 samples had non-detectable expression. (F) qPCR analysis of FACS sorted K5+ and K5- epithelial cells from *K5-venus* SMGs, $n = 3$ separate FACS analyses. Error bars show s.d. in (C) and (D). ANOVA, error bars show SEM in (E) and (F). * $p < 0.05$. nd = not detected. See also Figure S2.

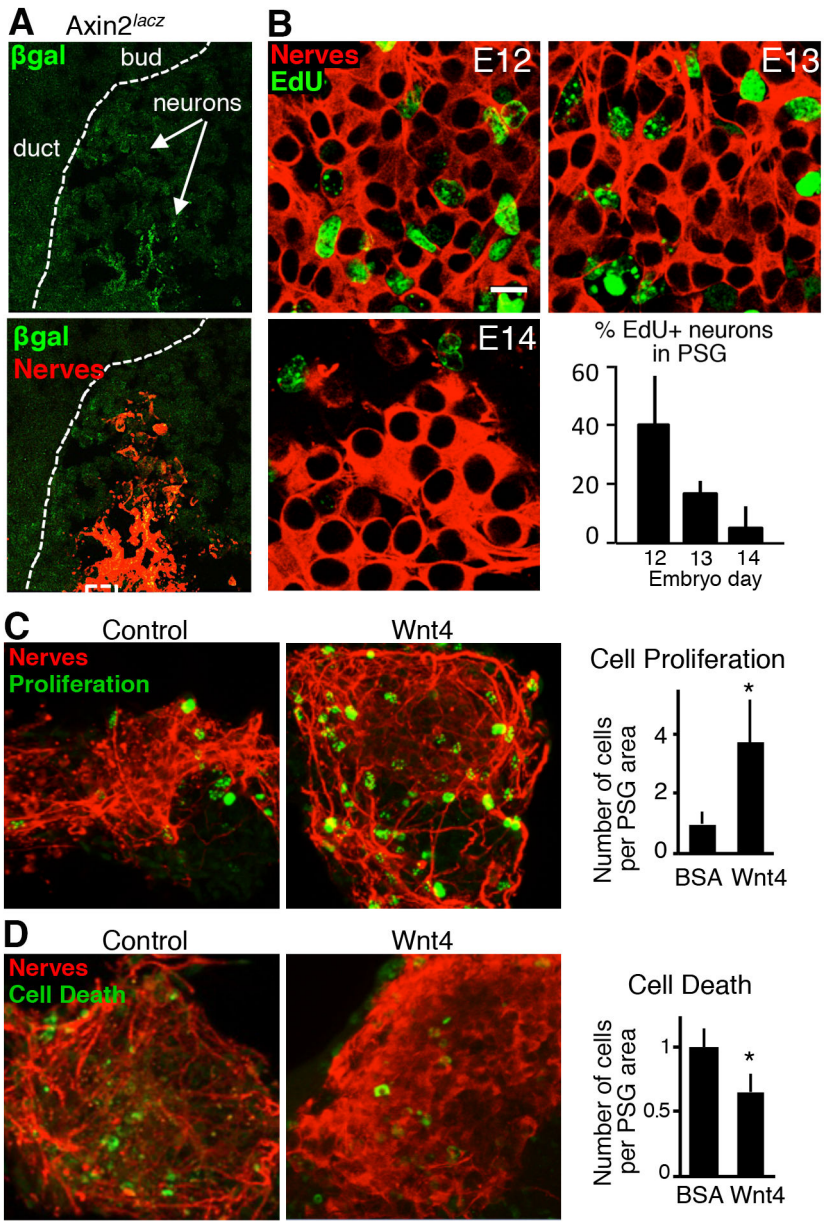

Figure 3. Wnt signaling promotes neuronal survival and proliferation in the PSG

(A) Immunostaining on cryosections of an E12 *Axin2*^{lacz} SMG for β-galactosidase (βgal) and nerves (Tubb3). White dashed lines outline the epithelium. Scale bar, 20 μm. (B) Wholemount immunostaining of E12, E13 and E14 SMGs for nerves and EdU to detect proliferating neurons in vivo. Graph depicts the quantitative analyses of proliferation (percent of EdU-positive neurons in the PSG). Scale bar, 5 μm. (C) E12 PSGs cultured for 24 h with BSA (control) or Wnt4 protein and immunostained for nerves and phospho-histone H3 (Proliferation) or caspase 3 (Cell death). Scale bar, 10 μm. (D) Quantitative analyses of proliferation and cell death in cultured PSGs. $n = 3$. Student's t test, error bars show s.d. * $p < 0.05$. See also Figure S3.

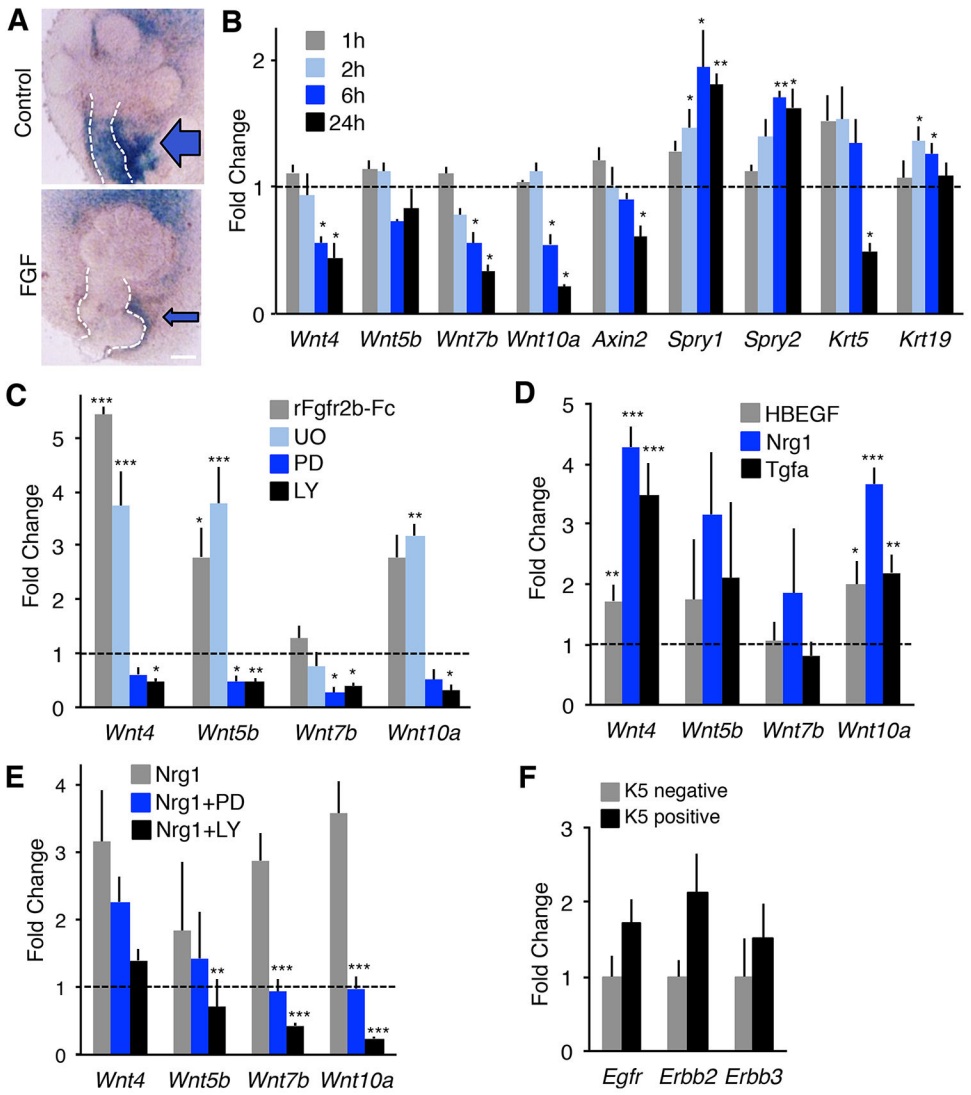

Figure 4. Wnt expression is negatively regulated by Fgfr2b signaling and upregulated by PI3K signaling downstream of erbB signaling

(A) E13 *Axin2*^{lacz} Control or FGF-treated SMGs stained with XGAL, *n* = 12. Blue arrows indicate periductal Wnt signaling. Scale bar, 100 μm. (B) qPCR timecourse of E12 SMGs treated with FGFs. *n* = 3 experiments. (C) Isolated E13 epithelia were treated for 4 h with 400 ng/ml FGF10 and either an Fgfr2b inhibitor (rFGFR2b-Fc, 25 nM), a MAPK inhibitor (U0126, UO, 20 μM), a pan-erbB inhibitor (PD168393, PD, 10 μM) or a PI3Kinase inhibitor (LY294002, LY, 25 μM). Gene expression of Wnt was normalized to DMSO or rFGFR1b-Fc (a control for rFGFR2b-Fc). Error bars show SEM. (D) Isolated E13 epithelia were treated with 20 ng/ml HBEGF, Nrg1, or Tgfα for 4 h. Wnt expression by qPCR was normalized to epithelia at 0 h. (E) Isolated E13 epithelia were treated for 2 h with 20 ng/ml Nrg1 + PD (10 μM) or LY (25 μM) and Wnt expression measured by qPCR and normalized to epithelia at 0 h. ANOVA compared to Nrg1 treated epithelia. None of the treatments affect morphogenesis within the 4 h time-points. (F) qPCR analysis of FACS sorted K5+ and K5- epithelial cells from *K5-venus* SMGs confirm K5+ cells express multiple erbB

receptors. *Egfr* (p = 0.10), *Erbb2* (p = 0.10), *Erbb3* (p = 0.49). *n* = 3. Error bars show SEM. Student's t test compared to BSA treated controls (B), rFGFR1b-Fc (C), and K5- cells (F). ANOVA compared to DMSO (C), epithelia at 0 h (D), and Nrg1 treated epithelia (E). * $p < 0.05$, ** $p < 0.01$, *** $p < 0.001$. See also Figure S4.

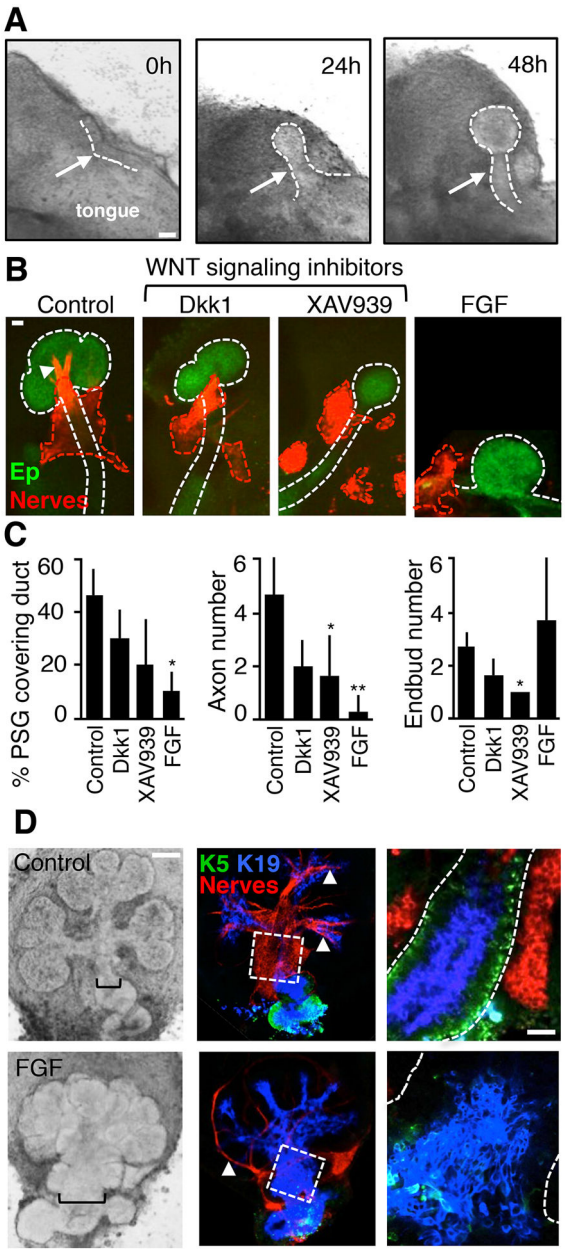

Figure 5. Inhibiting Wnt signaling impairs parasympathetic gangliogenesis, organ innervation and K5+ progenitor maintenance

(A) Whole mount brightfield images of a mandible culture timecourse. White arrows indicate the developing SMG; white dashed line outlines the developing SMG epithelium. Scale bar, 200 μm. (B) Immunostaining of control, Dkk1-, XAV939-, FGF-treated mandible cultures after 48 h. Ep is epithelium (E-cadherin) and nerves (Tubb3), n = 5–6 for each group. Dashed lines outline SMG epithelium (white) and ganglia (red), white arrowhead points to the axons. Scale bar, 50 μm. (C) Quantitation of the percentage of the PSG overlying the duct, the number of axons contacting the endbuds, and the total number of endbuds for each mandible treatment group. $n = 3$. ANOVA compared to control, error bars show s.d. * $p < 0.05$, ** $p < 0.01$. (D) E12 Control and FGF-treated SMGS, brightfield and

immunostaining for indicated markers, $n = 25$. Black brackets demarcate the width of the duct in the brightfield images. Dashed white boxes indicate the region of the duct imaged at 40X magnification in the lower panel; epithelial duct is outlined with a white dashed line. Scale bars, 100 μm for low power images and 25 μm for high power images. See also Figure S5.

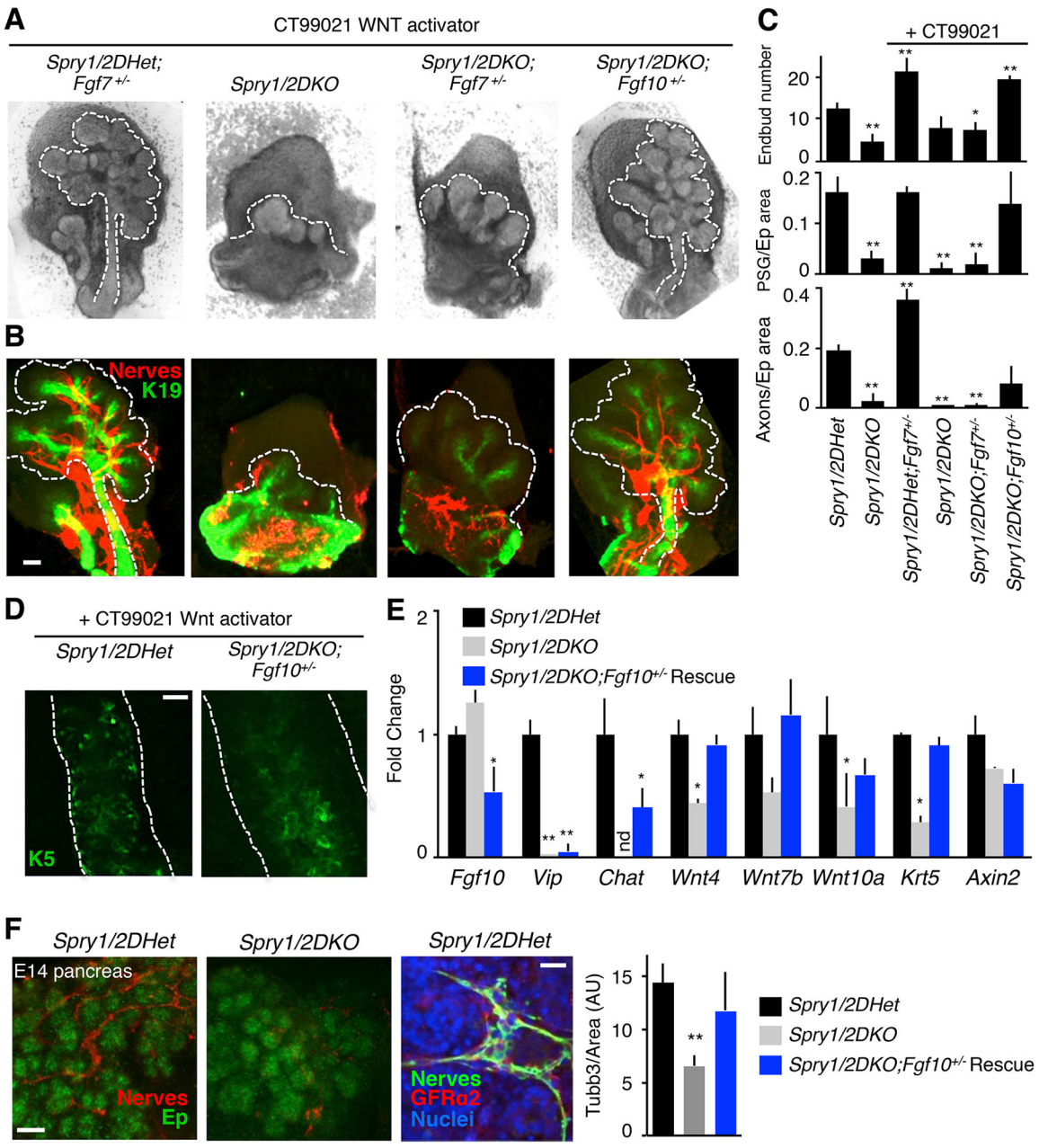

Figure 6. Increasing Wnt signaling while reducing FGF signaling rescues gangliogenesis and organ innervation in the Spry1/2 DKO SMG and pancreas in vivo

(A) Brightfield images of E14 SMGs from embryos treated with a single dose of CT99021 Wnt activator. *Spry1/2DHet;Fgf7*$^{+/-}$ (*n* = 7), *Spry1/2DKO* (*n* = 4), *Spry1/2DKO;Fgf7*$^{+/-}$ (*n* = 5), *Spry1/2DKO;Fgf10*$^{+/-}$ (*n* = 7). Scale bar, 100 μm. (B) Immunostaining of SMGs pictured in (A) for indicated markers. White dashed lines outline the glands. Scale bar, 100 μm. (C) Quantitation of endbud number, relative PSG area and the number of axons normalized to epithelial area. *n* = 3 for each genotype and treatment. (D) K5 immunostaining of SMGs pictured in (A). Scale bar, 25 μm. (E) qPCR analysis of CT99021 treated SMGs. *n* = 10 controls, 4 mutants and 6 rescues for qPCR analyses. (F)

Immunostaining of E14 *Spry1/2DHet* and *Spry1/2DKO* pancreas for nerves (Tubb3) and epithelium (Ep, E-cadherin). Scale bar, 50 μm. *Spry1/2DHet* pancreas stained for nerves (Tubb3), GFRα2 and nuclei (Hoechst). Scale bar, 10 μm. Quantitation of innervation in CT99021 treated *Spry1/2DHet* (*n* = 4), *Spry1/2DKO*, (*n* = 5) and rescued *Spry1/2DKO;Fgf10*$^{+/-}$, (*n* = 5) pancreas. ANOVA, error bars show SEM (D), s.d. (E). * $p < 0.05$, **$p < 0.01$, nd = not detected. See also Figure S6.

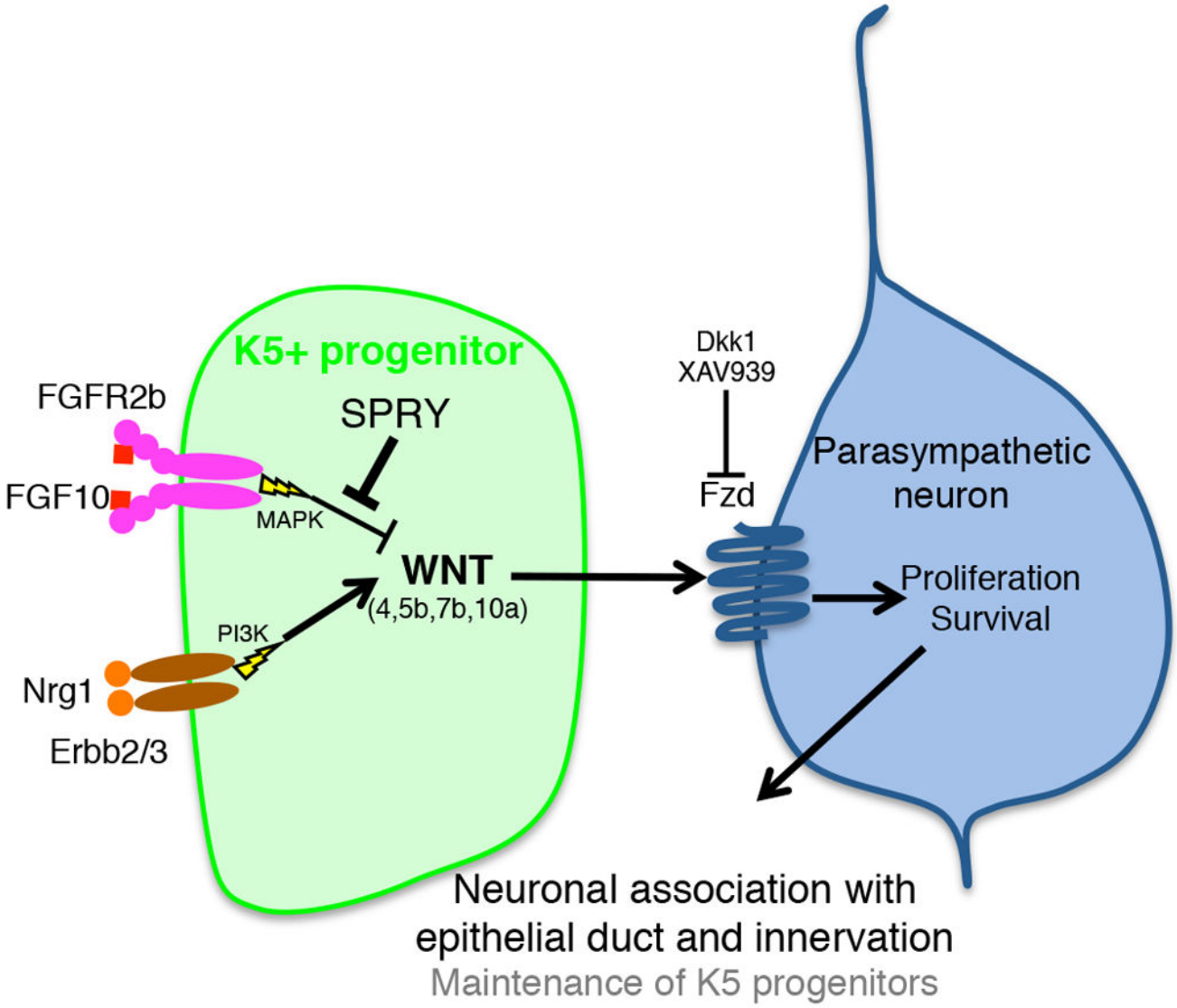

Figure 7. Model of SMG gangliogenesis

K5+ progenitor cells in the SMG duct produce Wnt ligands (Wnt4, 5b, 7b and 10a), which signal to adjacent parasympathetic neuronal cells. Wnt signals promote neuronal cell proliferation and survival, resulting in gangliogenesis, association with the epithelial duct and subsequent innervation. FGF signals inhibit Wnt expression and signaling, and Sprouty1 and Sprouty2 are required to restrict FGF signaling and allow Wnt expression. PI3K-dependent Nrg signaling positively regulates epithelial Wnt expression within K5+ cells. Subsequent ganglion function plays a key role in maintenance of K5+ progenitors required for organogenesis.